Gamma exposure from building materials – A dose model with expanded gamma lines from naturally occurring radionuclides applicable in non-standard rooms

Peer-reviewed author version

CROYMANS-PLAGHKI, Tom; Leonardi, Federica; Trevisi, Rosabianca; Nuccetelli, Cristina; SCHREURS, Sonja & SCHROEYERS, Wouter (2018) Gamma exposure from building materials – A dose model with expanded gamma lines from naturally occurring radionuclides applicable in non-standard rooms. In: CONSTRUCTION AND BUILDING MATERIALS, 159, p. 768-778.

DOI: 10.1016/j.conbuildmat.2017.10.051
Handle: http://hdl.handle.net/1942/25403

Gamma exposure from building materials – a dose model with expanded gamma lines from Naturally Occurring Radionuclides applicable in non-standard rooms.

Tom Croymans[1], Federica Leonardi[2], Rosabianca Trevisi[2], Cristina Nuccetelli[3], Sonja Schreurs[1], Wouter Schroeyers[1]
[1] Hasselt University, CMK, NuTeC, Nuclear Technology - Faculty of Engineering Technology, Agoralaan building H, B-3590 Diepenbeek, Belgium
[2] INAIL (National Institute for Insurance against Accidents at Work) - Research Sector, DiMEILA, Via di Fontana Candida 1 00078 Monteporzio Catone (Rome), Italy
[3] ISS (National Institute of Health), Technology and Health Department, Viale Regina Elena, 299, Rome, Italy
*Corresponding author: wouter.schroeyers@uhasselt.be
Tel: +3211 29 21 57
* Hasselt University, NuTeC, CMK, Nuclear Technology - Faculty of Engineering Technology, Agoralaan building H, B-3590 Diepenbeek, Belgium

Keywords
Euratom Basic Safety Standards; Dose Models; Naturally Occurring Radionuclides; Naturally Occurring Radioactive Materials; Radioactivity; Building materials; Concrete; Inorganic polymers; Alkali-activated materials; External gamma exposure

Abstract

Building materials are a significant source of gamma rays exposure due to the presence of naturally occurring radionuclides. In order to protect the public from harmful radiation, the European Basic Safety Standards (Council directive 2013/59/Euratom) introduced a one-size-fits-all building(s) (materials) Activity Concentration Index (ACI) based on a limited set of gamma lines. The ACI is considered *"as a conservative screening tool for identifying materials that may cause the reference level (i.e. 1 mSv/y) laid down in Article 75(1) to be exceeded".* Regarding calculation of dose, many factors such as density and thickness of the building material, as well as factors relating to the type of building, and the gamma emission data need to be taking into account to ensure accurate radiation protection. In this study the implementation of an expanded set of 1845 gamma lines, related to the decay series of ^{238}U, ^{235}U and ^{232}Th as well as to ^{40}K, into the calculation method of Markkanen [1], is discussed. The expanded calculation method is called the Expanded Gamma Dose Assessment (EGDA) model. The total gamma emission intensity increased from 2.12 to 2.41 and from 2.41 to 3.04 for respectively the ^{238}U and ^{232}Th decay series. In case of ^{40}K a decrease from 0.107 to 0.1055 is observed. The ^{235}U decay series is added, having a gamma emission intensity of 3.1. In a standard concrete room, the absorbed dose rates in air (D_A) per unit of activity concentration of 0.849, 0.256, 1.08, 0.0767 nGy/h per Bq/kg are observed. The use of weighted average gamma lines increased the D_A with 6.5 % and 1 % for respectively the ^{238}U and ^{232}Th decay series. A decrease of 4.5 % is observed in the D_A of ^{235}U decay series when using the weighted average gamma lines in comparison to its non-averaged variant. The sensitivity of the EGDA model for density, wall thickness, presence of windows and doors and room size is investigated. Finally, a comparison of the index and dose calculations relevant for the dose

assessment within the European legislative framework applicable towards building materials is performed. In cases where the ACI and density and thickness corrected dose calculation of Nuccetelli et al. [2] cannot provide guidance, the EGDA allows performing more accurate dose assessment calculations leading to effective doses which can be several 100 µSv/y lower.

1. Introduction

Building materials are a significant source of indoor gamma dose [3]. The importance to address the exposure originating from building materials is underlined in article 75 of the Euratom basic safety standards (EU-BSS) (Council directive 2013/59/Euratom) which comes into force in February 2018 [4]. This article states that "*The reference level applying to indoor external exposure to gamma radiation emitted by building materials, in addition to outdoor external exposure, shall be 1 mSv per year*". This European legislation was developed to establish basic standards, applicable in EU member states, for the protection against exposure of ionising radiation for workers and the general public. In a broader context this legislation supports several launched initiatives of the European commission for turning waste into a resource and promoting re-use and recycling with focus on the building industry in the framework of the Europe 2020 strategy [5–7]. In this context the EU-BSS aims towards a safe use of by-products, originating from NORM (Naturally Occurring Radioactive Material)-processing industries, like metallurgical slags, fly and bottom ash, phosphogypsum and red mud. These residues are used or investigated to use in cement-based matrixes as supplementary cementitious materials (SCM) on a large scale [8–12]. In addition more and more research is conducted to use these residues in more CO_2-friendly cement alternatives, like inorganic polymers (IPs) [8–10]. This fits with the aim to reduce the usage of primary resources. It is expected that future building materials used for dwellings will shift more and more towards these secondary raw materials that can potentially be rich in naturally occurring radionuclides (NORs): therefore the impact on the external gamma exposure of the use of these secondary raw materials needs to be assessed [10,13,14].

In order to assess the impact on external gamma exposure of building materials, different calculation methods, based on Monte Carlo simulations, integration and simple index and dose formulas, have been developed in the past [1,15–26]. Different dose assessment calculations have been developed based on gamma ray attenuation and build-up factors [1,16,17,22,27]. These calculations allow specifying the physical parameters of the room and the material it is constructed out, in a straightforward way. The density and wall thickness are identified as the most critical parameters. Modifying these parameters, for the evaluation of non-standard rooms, can generate dose rate differences up to 40 % compared to a standard concrete room [27]. Seeking for a standardized approach, the EU-BSS proposes a screening index, named Activity Concentration Index (ACI) [2]. This index was originally developed by Markkanen [1] and is described in the technical guide Radiation Protection (RP)-112 [28]. The ACI is based on a number of assumptions that are not all necessarily valid. The ACI assumes a concrete room (400 cm x 500 cm x 280 cm) with a density of 2350 kg/m^3 and thickness of 20 cm for all surfaces (walls, floor and ceiling). In the last years, in order to get a reliable screening tool, that will allow for a realistic discrimination of building materials, a new density and thickness corrected index I(ρd) was developed by Nuccetelli et al. [2]. The available dose assessment models focus on the standard composition of concrete, however the increased usage of residues, which have an *a priori* chemical compositions differing from conventional raw materials (like OPC and gravel), can result in structures with very different compositions. Some models consequently apply a correction factor to compensate for the different composition [29]. In addition, disequilibrium in the ^{238}U and ^{232}Th decay series chain can be present for residues from NORM-processing industries. Information regarding disequilibrium can be valuable for gaining insight into environmental or industrial processes. However, when dealing with the dose assessments of building materials one should assess how meaningful the consideration of disequilibrium is. Up to now, to the authors' knowledge, in none of the existing dose calculations, disequilibrium situations are taken into account. In contrast RP-122 [30]suggests using the highest activity concentration of a radionuclide present in a certain decay series to specify the activity concentration of that whole decay series. In none of the existing tools the presence of ^{235}U and its decay products is considered.

The above mentioned calculation methods have in common that they only use a fraction of the gamma emission lines known today. In practice, this means that often dose models use a specific set of major gamma lines or that the set of several major gamma lines is reduced to one or several averaged gamma lines with the gamma intensity as weighing factor. Whereas the gamma emission intensity of this averaged gamma line is the sum of the individual gamma emission intensities. This technique is performed to provide simplicity. However progress has been made in the characterization of the gamma emissions of radionuclides. The Laboratoire National Henri Becquerel has built an online database providing continuously updated information on the gamma emission lines of a wide range of radionuclides that allows going beyond this simplified approach [31]. Implementation of this database into a dose calculation method allows a more accurate safety assessment to evaluate if construction products can be used from a radiation protection point of view [2]. Both sample parameters, like density and composition, as well as room parameters like thickness of the walls, ceiling and floor, number of walls present, the sample composition of each wall etc. impact the final received dose [15,27]. An adaptable dose assessment calculation allows taking these parameters into account.

Using an flexible dose or index calculation, in contrast to a screening index, for the evaluation of building materials fits better with the 1 mSv dose requirement of article 75 of the EU-BSS [2], in particular when dealing with non-standard room and building material parameters. In addition the implementation of non–standard room and building material parameters deals with the requirement of annex VII of the EU-BSS, that states "*The calculation of dose needs to take into account other factors such as density, thickness of the material as well as factors relating to the type of building and the intended use of the material (bulk or superficial)*". The current study implements improvements, based on scientific data available in literature, into the existing and validated Markkanen room model. A sensitivity analysis of the different parameters impacting the calculated absorbed dose rate in air is performed. For the different improvements implemented in the dosimetric evaluation the impact and practicality for industrial implementation is discussed.

2. Materials & Methods

2.1 Materials

For the evaluation of the dose model the composition of concrete, defined by NIST [32], is used, except when mentioned differently.

2.2 Model

2.2.1 Model description

To assess the absorbed dose rate in air (D_A), the room model of Markkanen [1] (see Equation 1) is used.

$$D_A = 5.77\text{x}10^{-7}\,\frac{AC\,\rho}{4\pi}\sum \gamma_i \left(\frac{\mu_{en}}{\rho}\right)_i E_i \int B_i \frac{\mathrm{e}^{-\mu_i s}}{l^2}\mathrm{dV} \qquad (1)$$

With D_A the absorbed dose rate in air in Gy/h, *AC* the activity concentration of a radionuclide incorporated in the material of concern in Bq/kg, ρ the density of the material in kg/m^3, γ_i the gamma intensity of gamma line i, $(\mu_{en}/\rho)_i$ the energy absorption coefficient in air for gamma energy E_i in cm^2/g, E_i the photon energy in MeV, μ_i the linear attenuation coefficient of the material for gamma energy E_i in cm^{-1}, B_i the dose build up factor (see Equation 2) calculated via the Berger's formula, l the distance between the point of detection (x_p, y_p, z_p) and the point of integration in cm (see Equation 4) and *s* the fraction of l within the top layer in cm (see Equation 3). The total exposure rate is the sum of the exposure rates calculated from ceiling, floor and each wall. The $(\mu_{en}/\rho)_i$ is a polynomial best fit achieved from the data reported by Martin [33] using the data of Hubbell and Seltzer [34].

$$B_i = \; 1 + C(E_i)\mu_i s e^{D(E_i)\mu_i s} \qquad (2)$$

In literature different *C* and *D* parameters are proposed by different authors. In the model described here, the values of *C* and *D* proposed by Pelliccioni [35] are used. These are calculated for the energy spectrum via logarithmic and exponential best-fit function respectively by using the concrete parameters described by Pelliccioni [35] at 7 mean free paths (mfp).

$$s = \; \left|\frac{z}{z_p - z}\right| l \qquad (3)$$

$$l = \; \sqrt{(x_p - x)^2 + (y_p - y)^2 + (z_p - z)^2} \qquad (4)$$

In order to convert the D_A to effective dose a conversion factor of 0.7 Sv/Gy is used [28]. This conversion factor is used for all gamma emitters and originates from the UNSCEAR 2000 report [3].–This conversion factor is used in the dose calculations considered in this article and is consequently used for comparison reasons. Nevertheless, nuclide specific conversion factors have been suggested by Krstic and Nikezic [36].

The model assumes a homogeneous sample composition and a homogeneous distribution of the radionuclides throughout the composed materials. In addition a standard room is used as a reference throughout the paper. The standard room size was described by Koblinger [15] as measuring 400 cm x 500 cm x 280 cm. Here a standard thickness of walls, floor and ceiling of 20 cm is assumed. Neither doors nor windows are present and the point of detection (x_p, y_p, z_p) is set at the middle of the room. Whereas Koblinger suggested a density of 2320 kg/m^3, RP-112 suggests a density of 2350 kg/m^3 [15,28]. The value of 2350 kg/m^3 is used here as a standard.
No background correction is assumed when calculating the D_A.

All calculations are performed by a combination of Microsoft® excel and R® [37]. The input parameters are submitted in Microsoft® excel whereas the further treatment of the input data is performed by Microsoft® excel and R®.

2.2.2. Selection of the number of gamma lines

In order to check the impact of the number of gamma lines, a comparison of the absorbed dose rate in air is made between different dose assessment models for a standard room. The Markkanen [1], Mustonen [22], ISS room model [23] and the model developed in this study, further called Expanded Gamma Dose Assessment (EGDA) model, are compared. Different versions of the EGDA model are evaluated depending on the number of gamma lines used for the dose assessment. 'EGDA>1%', 'EGDA>0.1%', 'EGDA>0%' take into account all gamma lines which have a gamma emission intensity (including the branching factor) above respectively 1 %, 0.1 % and 0 % when considering gamma emission lines from the ^{238}U, ^{232}Th and ^{235}U decay series and ^{40}K. In addition two variants of 'EGDA>0.1%' are discussed. In one variant the emission gamma lines of ^{238}U and ^{232}Th (except for the 2614 keV gamma emission line since this emission line represents over 40 % of the dose rate of the ^{232}Th decay series) of 'EGDA>0.1%' are converted to one weighted average gamma emission line. This variant is indicated in Table 1 by the suffix "averaged". In the second variant the emission gamma lines which have a gamma emission intensity lower than 0.1 % are converted to one weighted average gamma line for ^{238}U, ^{232}Th and ^{235}U. This variant is indicated in Table 1 as "EGDA+". Details on each model are provided in Table 1. Since not all the details necessary for the calculations were present in the original paper of Markkanen [1] and Mustonen [22], updated values were used (details in Table 1). This is indicated by a suffix "updated". In addition, a second variant of the ISS room model, which makes use of the Berger parameters described by Pelliccioni [35] instead of the Berger parameters of Markkanen [1], is discussed. This variant is indicated with the infix "Pelliccioni" whereas the original ISS room model is indicated with the infix "original". For readability, abbreviations of the dose model names are provided in Table 1 and Table 5.

Table 1: Overview of the different dose calculation models and their parameters used to evaluate the absorbed dose rate in air.

Model	**Markkanen original**	**Markkanen updated**	**Mustonen updated**	**ISS original room model**	**ISS Pelliccioni room model**	**EGDA>1%**	**EGDA>0.1%**	**EGDA>0.1% averaged**	**EGDA+**	**EGDA>0%**
Concrete composition	Markkanen 1995 [1]	Ordinary Portland concrete (NIST)	Ordinary Portland concrete (NIST)	Ordinary Portland concrete (NIST)	Ordinary Portland concrete (NIST)	Ordinary Portland concrete (NIST)	Ordinary Portland concrete (NIST)	Ordinary Portland concrete (NIST)	Ordinary Portland concrete (NIST)	Ordinary Portland concrete (NIST)
Energy absorption coefficient in air	Markkanen 1995 [1]	Best fit from Martin 2006 [33]	Best fit from Martin 2006 [33]	Hubbell 1982 [38]	Hubell 1982 [38]	Best fit from Martin 2006 [33]	Best fit from Martin 2006 [33]	Best fit from Martin 2006 [33]	Best fit from Martin 2006 [33]	Best fit from Martin 2006 [33]
Density (kg/m3)	2350	2350	2350	2350	2350	2350	2350	2350	2350	2350
Linear attenuation coefficient	From Markkanen 1995 [1]	XCOM [39]: ordinary Portland concrete (NIST)	XCOM [39]: ordinary Portland concrete (NIST)	Hubbell 1982 [38]	Hubbell 1982 [38]	XCOM [39]: ordinary Portland concrete (NIST) or IP	XCOM [39]: ordinary Portland concrete (NIST) or IP	XCOM [39]: ordinary Portland concrete (NIST) or IP	XCOM [39]: ordinary Portland concrete (NIST) or IP	XCOM [39]: ordinary Portland concrete (NIST) or IP
Gamma emission energy and intensity	Markkanen 1995 [1]	Mustonen 1984 [22]	Mustonen 1984 [22]	NuDat website [40]	NuDat website [40]	DDEP website [31]	DDEP website [31]	DDEP website [31]	DDEP website [31]	DDEP website [31]
Berger Parameters	Markkanen 1995 [1]	Best fit of Pelliccioni 1989 [35]	Best fit of Pelliccioni 1989 [35]	Best fit of Markkanen 1995 [1]	Best fit of Pelliccioni 1989 [35]	Best fit of Pelliccioni 1989 [35]	Best fit of Pelliccioni 1989 [35]	Best fit of Pelliccioni 1989 [35]	Best fit of Pelliccioni 1989 [35]	Best fit of Pelliccioni 1989 [35]
Number of gamma lines ^{238}U	1	1	24	19*	19*	82	87	1*	87 + 1**	761
Gamma emission intensity ^{238}U* **	2.12	2.12	2.12	2.41	2.41	2.19	2.36	2.36	2.41	2.41
Number of gamma lines ^{232}Th	2	2	20	14*	14*	36	110	2*	110 + 1**	349

Gamma emission intensity ^{232}Th* **	2.41	2.41	2.41	2.63	2.63	2.76	2.98	2.98	3.04	3.04
Number of gamma lines ^{40}K	1	1	1	1	1	1	1	1	1	1
Gamma emission intensity ^{40}K	0.107	0.107	0.107	0.107	0.107	0.1055	0.1055	0.1055	0.1055	0.1055
Number of gamma lines ^{235}U	-	-	-	-	-	47	128	1*	128 + 1**	734
Gamma emission intensity ^{235}U* **	-	-	-	-	-	2.78	3.04	3.04	3.1	3.1
Model abbreviation	Mark$_{orig}$	Mark$_{upd}$	Must$_{upd}$	ISS$_{orig}$	ISS$_{Pelli}$	-	-	-	-	-

* 87, 109 and 128 gamma emission lines are converted to 1 for respectively ^{238}U, ^{232}Th and ^{235}U

** 674, 239 and 606 gamma emission lines are converted to 1 for respectively ^{238}U, ^{232}Th and ^{235}U

*** The gamma emission intensity is the sum of the individual gamma-ray emission energies.

2.2.3. Role of the build-up factor

The impact of the build-up factor (B) was evaluated for a standard room by using different sets of Berger parameters C and D to calculate the D_A per unit of activity concentration. The Berger parameters as described by Markkanen and by Pelliccioni were compared [1,35]. In addition the case without Berger parameters (C=D=0) is evaluated, meaning the role of build-up factor is neglected. The latter case is indicated by the suffix “B = 1” in Table 4.

2.2.4. Role of the presence disequilibria in the ^{232}Th, ^{238}U and ^{235}U decay series

For model ‘EGDA>0.1%’ the contribution of long living radionuclides and their progeny to the total absorbed dose rate in air per unit of activity concentration for the decay series of ^{238}U and ^{232}Th is evaluated. The ^{238}U decay chain is divided into 3 subchains : i.e. ^{238}U-part (^{238}U to ^{230}Th), ^{226}Ra-part (^{226}Ra to ^{214}Po) and ^{210}Pb-part (^{210}Pb to ^{210}Po). Similar, the ^{232}Th decay chain is divided into ^{232}Th-part (only ^{232}Th), ^{228}Ra-part (^{228}Ra to^{228}Ac) and ^{228}Th-part (^{228}Th to ^{208}Tl). The absorbed dose rate in air of ^{235}U is evaluated in the framework of the ratio of AC of ^{238}U/^{235}U i.e. 21.6 as expected value for non- diluted/enriched samples. No disequilibrium is considered in case of ^{235}U decay series as (dis)equilibrium in this decay series is often not reported.

2.2.5 Impact of sample specific composition

The impact of the sample composition on the dose rate is compared by simulating a room constructed out of Fayalite Slag based Inorganic Polymers (FSIPs). FSIPs have different chemical, physical and structural properties than concrete. The characteristics of FSIPs are described by Kriskova et al. [41], Onisei et al. [42] and Iacobescu et al. [43]. The sample composition differs from concrete consequently leading to the usage of different linear attenuation coefficients. The attenuation coefficients are calculated for each gamma emission energy via the XCOM program [44]. The sample specific coherent mass attenuation coefficient of XCOM is therefore converted to the sample specific linear attenuation coefficient.

2.3. Sensitivity Analysis

A sensitivity analysis of the parameters impacting the absorbed dose rate in air is performed. The studied parameters are density, wall thickness, presence of windows and doors and room size. All parameters are compared to the standard parameters of a standard concrete room as defined in section 2.2.1.

2.3.1. Density

The impact of the wall density on the D_A is tested for a standard room with density varying stepwise (step size of 100 kg/m^3) between 1000 kg/m^3 and 3500 kg/m^3, corresponding to the density of hollow bricks up to the density of high density concrete.

2.3.2. Wall Thickness

In a standard concrete room the wall thickness is assumed to be 20 cm. However depending on the usage thinner or thicker walls are required. The impact of the wall thickness on the D_A in the standard room is tested with wall thickness varying stepwise (step size of 5 cm) between 5 cm and 80 cm while keeping floor and ceiling thickness constant at 20 cm.

2.3.3. Room Size

The impact of the room size on the D_A is tested for a concrete room. A square room is simulated with length of the wall varying stepwise (step size of 100 cm) between 100 cm and 1000 cm for a room height of 280 cm and between 100 cm and 1183.2 cm for a room height of 200 cm.

2.3.4 Presence of windows and doors

The EU-BSS assumes a standard room without the presence of windows and doors. This is a strict approach but not realistic. The impact of the presence of windows or doors of different surfaces is tested. Tests are conducted for surfaces of 1 m^2, 2 m^2 and 4 m^2 positioned in the middle or the corner of a wall or ceiling. The imaginary dose rate originating of the specific window/door surface is subtracted from the dose rate of the wall without any window/door.

2.4 Comparison of index and dose assessment tools

A comparison is made of the most used index and dose calculations relevant for the dose assessment within the European legislative framework applicable towards building materials. More details regarding these different index and dose calculations are shown in Table 2 or can be found in the respective references.

The index values calculated via ACI and the density and thickness corrected index (I(ρd)) are compared using the AC of different types of residues and cement shown in Table 3 [1,2,4]. The obtained dose of the Markkanen original, density and thickness corrected (D(ρd)) and EGDA>0% dose calculations are compared using the same AC [1,2,30]. In addition to the standard density of 2350 kg/m^3 and standard thickness of 20 cm, six different scenarios are tested with varying density and thickness (Table 4). In the comparisons, it is assumed that the residues are solely used to construct a building material, this because recent studies [45,46] indicate the applicability of building materials without the use of any additives like cement, sand, gravel, etc. The AC values originate from Nuccetelli et al. [10]. In all cases the exposure time is 7000 h.

Table 2: Overview of the parameters of the index and dose calculations used in the European legislative framework applicable towards building materials.

	Index calculation		**Dose calculation**		
	ACI	**I(ρd)**	**Markkanen original**	**D(ρd)**	**EGDA>0%**
Geometry	Floor, ceiling, 4 walls	Floor, ceiling, 4 walls	Floor, ceiling, 4 walls	Floor, ceiling, 4 walls	Floor, ceiling, 4 walls
Size geometry (cm^3)	400 x 500 x 280*	400 x 500 x 280	400 x 500 x 280	400 x 500 x 280	(Flexible) Here 400 x 500 x 280
Wall thickness (cm)	20	Flexible	20	Flexible	Flexible
Density (kg/m^3)	2350**	Flexible	2350**	Flexible	Flexible
Background correction	70 nGy/h	50 nGy/h	0.348 mSv	0.245 mSv	0.245 mSv

Composition	Concrete	Concrete	Concrete	Concrete	(Flexible) Here Concrete
Reference(s)	EC 2014; RP112; Markkanen 1995	Nucetelli et al. 2015	EC 2014; RP112; Markkanen 1995	Nucetelli et al. 2015	

* In Markkanen 1995 size is 12 x 7 x 2.8 m^3 with thickness of 0.2 m

** In Markkanen 1995 density is 2320 kg/m^3

Table 3: Activity concentrations (Bq/kg) of ^{226}Ra, ^{232}Th and ^{40}K present in different residues and cement.

Material type	^{226}Ra (Bq/kg)	^{232}Th (Bq/kg)	^{40}K (Bq/kg)	Reference
Furnace slags *	147	42	258	Nuccetelli et al. 2015
Bottom ash and fly ash *	207	80	546	Nuccetelli et al. 2015
Phosphogypsum *	381	22	71	Nuccetelli et al. 2015
Bauxite residue *	337	480	205	Nuccetelli et al. 2015
Cement *	42	32	214	Nuccetelli et al. 2015

* Average values of database from Nuccetelli et al. 2015 [10]

Table 4: Description of 6 different scenarios which are described by a specific set of density and thickness. The scenarios are used for the comparison of the models of Table 2.

Scenario number	1	2	3	4	5	6
Thickness (cm)	10	10	18	25	40	40
Density (kg/m^3)	1400	3000	3000	1400	1400	3000

3. Results and discussion

In section 3.1 the different absorbed dose rates in air per unit of activity concentration for ^{238}U, ^{232}Th, ^{40}K and ^{235}U obtained by different dose assessment models are compared. This section discusses the impact of working with averaged gamma emission lines as well as the impact of the build-up factor and the radiological equilibria.

Based on this comparison, the most practical EGDA model with the highest gamma emission intensity is selected and in section 3.2 a sensitivity analysis of this model is performed by changing wall thickness and density, room size and the presence of windows and doors. Throughout section 3.1 and 3.2 the impact of the sample composition is quantified.

Section 3.3 deals with the application of the model focussing on the dosimetric evaluation, the impact and the practicality for industrial implementation. Consequently a comparison is performed of the most used index and dose calculations relevant for the dose assessment within the European legislative framework applicable towards building materials.

3.1. Model

3.1.1. Impact of the number of gamma lines

Table 5 shows the D_A per unit of activity concentration for ^{238}U, ^{232}Th, ^{40}K and ^{235}U of the different models described in Table 1. The different models assume a concrete standard room unless indicated else by suffix FSIP.

Table 5: Overview of the absorbed dose rate in air per unit of activity concentration (nGy/h per Bq/kg) for ^{238}U, ^{232}Th, ^{40}K and ^{235}U calculated by different dose assessment calculation models described in Table 1.

	^{238}U	^{232}Th	^{40}K	^{235}U
Model abbreviation	**Dose rate in air (D_A) (nGy/h per Bq/kg)**	**Dose rate in air (D_A) (nGy/h per Bq/kg)**	**Dose rate in air (D_A) (nGy/h per Bq/kg)**	**Dose rate in air (D_A) (nGy/h per Bq/kg)**
$Mark_{orig}$	0.908	1.06	0.0767	-
$Mark_{orig\ B=1}$	0.3845	0.5	0.0408	-
$Mark_{upd}$	0.893	1.02	0.0778	-
$Mark_{upd\ B=1}$	0.383	0.501	0.0407	-
$Must_{upd}$	0.84	0.999	0.0778	-
$Must_{upd\ B=1}$	0.0405	0.51	0.0407	-
ISS_{orig}	0.894	1.138	0.0767	-
ISS_{Pelli}	0.869	1.109	0.0767	-
EGDA>1%	0.76	0.967	0.0767	0.228
EGDA>0.1%	0.826	1.06	0.0767	0.25
EGDA>0.1% $_{B=1}$	0.395	0.535	0.0401	0.0819
EGDA>0.1% FSIP	0.838	1.07	0.0784	0.234
EGDA>0.1%$_{aver}$	0.88	1.07	0.0767	0.239
EGDA>0.1%$_{aver\ B=1}$	0.368	0.51	0.0401	0.0725
EGDA+	0.85	1.08	0.0767	0.255
EGDA>0%	0.849	1.08	0.0767	0.256

Suffix ‘orig’ (original): Data of the original paper are used as shown in Table 2.
Suffix ‘upd’ (updated): Updated data, as shown in Table 2, are used with the original calculation method.
Suffix ‘B=1’ (build-up factor = 1): The Berger parameters are set to zero. This means the role of the build-up factor is negligible.
Suffix ‘aver’ (averaged): Several gamma lines are reduced to a single weighted average gamma emission line.
Suffix ‘Pelli’ (Pelliccioni): the Berger parameters as described by Pelliccioni 1989 are used.
FSIP: The chemical composition of the room components is set to the FSIP chemical composition.

Comparing the D_A between $Mark_{orig}$ and $Mark_{upd}$, an increase of 1.7 % and 3.8 % is observed for respectively ^{238}U and ^{232}Th, in favour of the $Mark_{orig}$ model. In case of ^{40}K a decrease of 1.4 % is observed in favour of the $Mark_{orig}$ model. This deviation in D_A is due to the usage of different Berger parameters and a different concrete composition in the two models (Table 1).

The 24 emission gamma lines of ^{238}U and the 19 gamma emission lines (2614 keV-line is excluded) of ^{232}Th of the Mustonen model are converted to a single weighted average gamma emission line for ^{238}U and ^{232}Th in the Markkanen model.
Comparing $Mark_{upd}$ with $Must_{upd}$ a 6 % and 2 % increase in D_A is observed for respectively ^{238}U and ^{232}Th. This increase is solely due to usage of averaged gamma lines in the Markkanen model. In case of ^{235}U a decrease in the D_A of 4.6 % (4.9 %) is observed for the 'averaged EGDA' variant. The differences are solely due to the usage of energy specific attenuation coefficients and energy specific C and D Berger parameters as the total gamma intensity stays equal.

When comparing the EGDA models with $Mark_{upd}$, $Must_{upd}$ and the ISS room models one can see that the number of gamma lines used is much higher (Table 1). When more gamma lines are included in the EGDA model the gamma emission intensity also increases for ^{238}U, ^{232}Th and ^{235}U, leading to higher D_A when comparing EGDA>1%, EGDA>0.1% and EGDA>0%. However the gamma emission intensity of the ISS room model is smaller than the gamma emission intensity of EGDA>0% for ^{238}U and ^{232}Th (Table 1), still the D_A of the ISS room model is higher than the D_A of EGDA>0% (Table 5). The usage of a set of averaged gamma-lines in the ISS room models tends to increase the D_A, as discussed above. In addition the usage of other B in the ISS_{orig} (Table 1) also impacts the D_A, this is discussed in section 3.1.2.

The EGDA>0% model uses all the gamma lines available originating from ^{238}U, ^{232}Th, ^{235}U and ^{40}K. In total 1845 gamma lines are used in the calculation by model EGDA>0% whereas in model EGDA>0.1% 326 gamma lines are used. The gamma emission intensity of EGDA>0.1% is 2.1 %, 2.0 % and 1.9 % lower than EGDA>0% for respectively ^{238}U, ^{232}Th and ^{235}U. Nevertheless, when using a higher number of gamma lines also the calculation time increases. In order to limit the calculation but still consider the maximum gamma emission intensity, the extra gamma lines of EGDA>0% in comparison to EGDA>0.1% are converted to 3 weighted average gamma lines; one line for ^{238}U, ^{232}Th and ^{235}U. This approach is incorporated in the EGDA+ model (Table 1). The difference in D_A between EGDA+ and EGDA>0% is limited to plus 0.001 nGy/h per Bq/kg for ^{238}U and minus 0.001 nGy/h per Bq/kg for ^{235}U. In case of ^{232}Th no difference was observed.

3.1.2. Impact of the Build-up factor

Table 5 shows the D_A for several models. Comparing the D_A of the "B=1" variants with the non-unity originals, a significant decreases in the D_A is present. For example in the case of EGDA>0.1% the "B=1" variant has an D_A which is approximately 52 %, 50 %, 48 % and 67 % lower for respectively ^{238}U, ^{232}Th, ^{40}K and ^{235}U. The presence of the B is consequently important when calculating the D_A. The ISS_{Pelli} model differs only from the ISS_{orig} model by the usage of the data of Pelliccioni instead of the data of Markkanen to calculate the B. Comparing both models, the D_A per unit of activity concentration of the ISS_{Pelli} model is 2.8 % and 2.6 % lower for respectively ^{238}U and ^{232}Th in case of a standard concrete room.

3.1.3. Impact of disequilibrium in the ^{232}Th, ^{238}U and ^{235}U decay series

Table 6: Absorbed dose rate in air (D_A) per unit of activity concentration (nGy/h per Bq/kg) of the long-living radionuclides and their progeny of the ^{238}U and ^{232}Th decay series in case of the EGDA>0.1% model.

Concrete standard room					
^{238}U Decay series			**^{232}Th Decay series**		
	D_A (nGy/h per Bq/kg)	**% Contribution**		**D_A (nGy/h per Bq/kg)**	**% Contribution**
^{238}U Part	0.0077	0.931	**^{232}Th Part**	0.000041	0.004
^{226}Ra Part	0.82	99.002	**^{228}Ra Part**	0.42	39.583
^{210}Pb Part	0.00055	0.067	**^{228}Th Part**	0.64	60.413

Considering the decay series of ^{238}U: the ^{238}U-part, ^{226}Ra-part and ^{210}Pb-part of the decay chain represent respectively approximately 0.93 %, 99 % and 0.067 % of the total external absorbed gamma dose rate in air per unit of activity concentration of the whole ^{238}U decay series, in the case of a standard concrete room. The lifespan of a building material will not allow reestablishing the equilibrium between the ^{238}U-part and ^{226}Ra-part. Looking solely at the lifespan aspect, it would be meaningful to treat both parts of the decay chain separately. However, this is not always feasible since one must be able to measure ^{238}U, ^{234}Th or ^{234}Pa. Using in this case the AC of ^{226}Ra for the whole decay series will only introduce a small bias since ^{238}U part and ^{210}Pb contribute less than 1 % to the total D_A of the ^{238}U decay series. On the other hand using the AC of ^{238}U for ^{226}Ra and its decay products would have a large impact as ^{226}Ra-part represents 99 % of the D_A of the ^{238}U decay series. The suggestion of RP-122 to use the highest AC present in the decay series would overestimate the gamma dose rate when the AC of ^{238}U or ^{210}Pb is larger than the AC of ^{226}Ra. Due to the small contribution of ^{210}Pb-part to the gamma dose (i.e. 0.067%), the activity concentration of ^{226}Ra is used for the ^{210}Pb-part of the decay series in this study. The half-life of ^{222}Rn allows radon exhalation from the building material which decreases the external absorbed gamma dose rate in air. De Jong and Van Dijck (2008) [18] showed that the external absorbed gamma dose rate in air decreased on average with 9 % and 5 % for respectively gypsum and concrete used in the Netherlands. In addition the EU-BSS [4] treats the radon exposure (from soil and building materials) separately from the gamma exposure linked to building materials. For this reason all the EGDA models do not consider radon and is therefore stricter in terms of gamma ray exposure.

Considering the decay series of ^{232}Th: the ^{232}Th-part, ^{228}Ra-part and ^{228}Th-part of the decay chain represent respectively approximately 0.004 %, 39.6 % and 60.4 % (Table 6) of the total external absorbed gamma dose rate in air per unit of activity concentration of the whole ^{232}Th decay series in the case of a standard concrete room. Disequilibria in the ^{232}Th decay chain are complex and insights in the production process of NORM-residues can provide useful information. In the case of complete Th-separation, the equilibrium will install within a timeframe of 40 years in the Th-bearing residue. Whereas in the Ra-bearing residue the activity will fade away. The lifetime of building materials can be considered to cover this timespan. Being strict, it is best not to consider disequilibrium and consider the highest activity concentration that is possible and use for the complete (so 100 %) D_A calculation of the ^{232}Th decay series. An adequate determination of the activity concentration is recommended to assess whether or not disequilibria are present. In addition it is assumed in this study that no ^{220}Rn exhalation from the building material takes place as the half-life of ^{220}Rn is relatively short (55.8 sec).

To the authors knowledge in none of current dose assessments tools available, the decay series of ^{235}U is considered. However taking into account all the gamma emission intensities above 0.1 % the absorbed dose rate in air is 0.250 nGy/h per Bq/kg for a standard concrete room (Table 5). This is above the D_A of ^{40}K on a Bq/kg level. However framing this ^{235}U D_A in a broader context, when the natural abundance of U is respected the AC of ^{235}U is 0.0463 times the AC of ^{238}U. So in reality the contribution of the D_A of ^{235}U is of limited consequence, except when high activity concentrations of ^{238}U are present. When no ^{235}U is measured, the authors recommend using 0.0463 times the AC of ^{238}U to implement the dose originating from ^{235}U. Within the ^{235}U decay series, disequilibrium situations can also be present but these are not considered here.

3.1.4. Impact of sample specific composition

The impact of the sample composition is studied by comparing EGDA>0.1% and EGDA>0.1% FSIP. An increase in the D_A of 1.4 %, 0.9 % and 2.1 % is observed for ^{238}U, ^{232}Th and ^{40}K when FSIP is used instead of concrete. On the contrary, in case of ^{235}U, a decrease in the D_A of 6.8 % is observed. It has to be noted that here solely the linear attenuation coefficients are changed. A change of sample composition implies also changing the energy and mfp-dependent B, due to the interdependency between the composition, the energy and the mfp. However, the study of this aspect is outside the scope of this paper.

3.1.5. Selection of EGDA>0% model

The EGDA>0% model uses the highest gamma emission intensity and makes use of all the nuclear data on an individual base. Consequently this approach is the more accurate one and is selected for the performance of a sensitivity analysis in section 3.2. ~~The use of 3 weighted gamma emission lines in case of ^{238}U, ^{232}Th and ^{235}U, corresponding to respectively 2.1 %, 2.0 % and 1.9 % of the total gamma emission intensity, allows performing faster calculations in comparison to EGDA>0% model.~~ The C and D Berger parameters described by Pelliccioni (1989) [35] are used for the calculations.
The presence of gamma emission by ^{235}U is considered and disequilibrium situations can be considered when necessary.

3.2. Sensitivity Analysis of EGDA>0% Model

3.2.1. Impact of the wall thickness calculated by the EGDA>0% model.

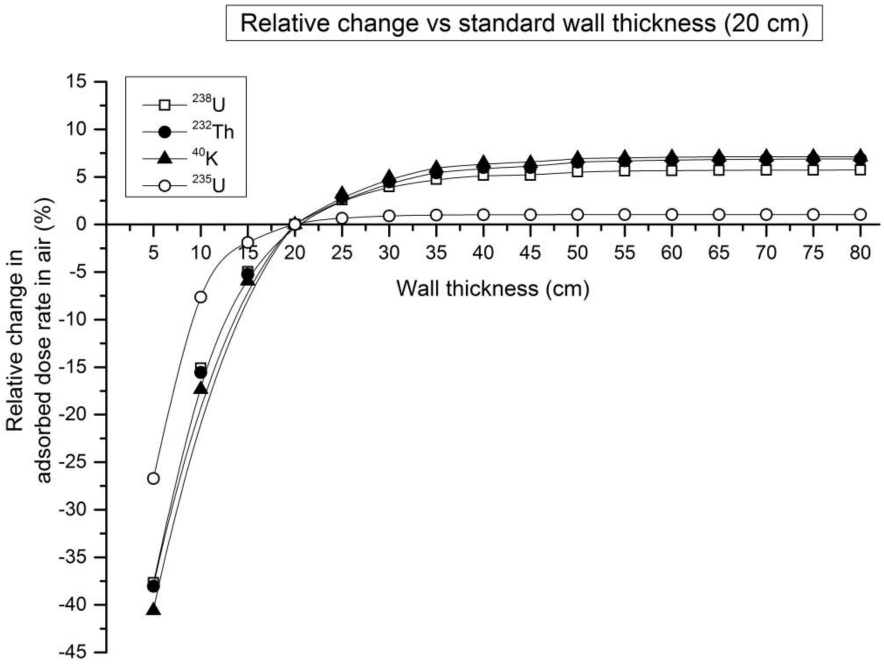

Figure 1: Relative change in the absorbed dose rate in air (D_A) for a standard concrete room with varying thickness (5-80 cm) vs a standard concrete room with wall thickness of 20 cm for ^{238}U, ^{232}Th, ^{40}K and ^{235}U. Relative change: ($D_A$thickness$_X$ –$D_A$thickness$_{20cm}$)/ ($D_A$thickness$_{20cm}$ x 100)

Figure 1 shows the relative change (%) in D_A air for different thicknesses relative to the wall thickness of 20 cm for ^{238}U, ^{232}Th, ^{40}K and ^{235}U in a standard concrete room. It is observed that the relative decrease in D_A occurs rapidly with decreasing wall thickness. In case of a wall thickness of 5 cm a relative decrease of 27.4 %, 27.6 %, 28.9 % and 21.1 % is observed for respectively ^{238}U, ^{232}Th, ^{40}K and ^{235}U. In case of a wall thickness of 80cm a relative increase of 6.1 %, 7.4 %, 7.7 % and 1.1 % is observed for respectively ^{238}U, ^{232}Th, ^{40}K and ^{235}U. However, a plateau in the increase of the D_A is observed. The percentage increase of the D_A between 20 cm and 25 cm thickness is below 1 % for ^{235}U whereas for the other radionuclides this is approximately 3 %. From a thickness of 40 cm, the increase in the D_A is below 1 % per increase in 5 cm thickness for all the radionuclides. According to Risica et al. (2001) [27] this plateau originates from self-absorption effects.

As the floor thickness is not varied the contribution of the walls to the D_A will increase with the thickness. The contribution of the smaller wall (400 cm) will increase with approximately 5 % relative to the larger wall (500 cm) when increasing the wall thickness from 5 cm to 80 cm.

3.2.2. Impact of the density calculated by EGDA0% model

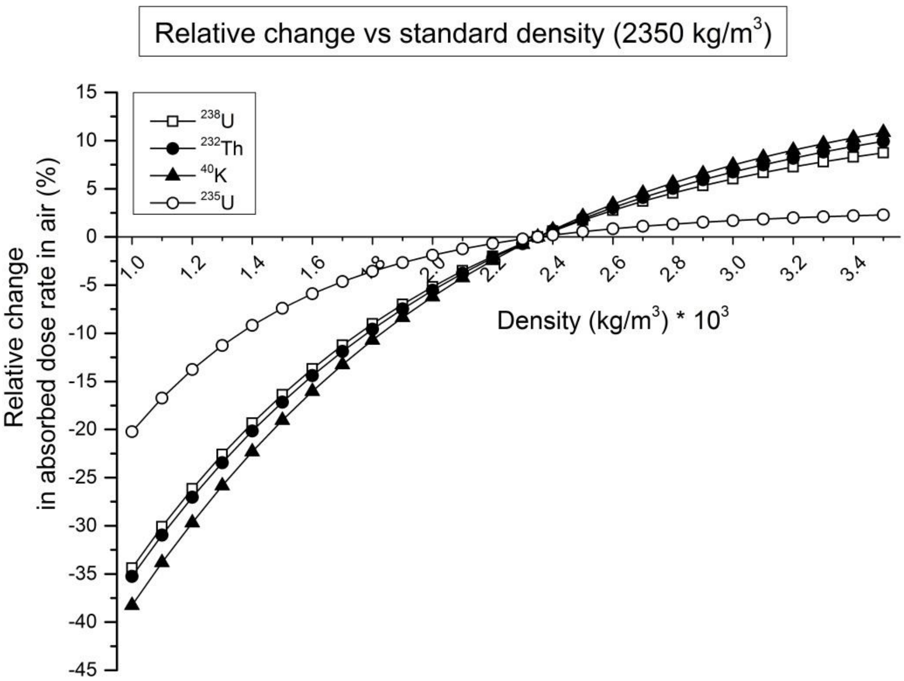

Figure 2: Relative difference of the absorbed dose rate in air (D_A) for a standard concrete room with varying density (1000-3500 kg/m^3) vs a standard concrete room with density of 2350 kg/m^3 for ^{238}U, ^{232}Th, ^{40}K and ^{235}U. Relative change: ($D_A$density$_X$ –$D_A$density$_{2350\ kg/m3}$)/ ($D_A$density$_{2350\ kg/m3}$ x 100)

Figure 2 shows the difference in D_A for different densities relative to the standard density of 2350 kg/m^3 for ^{238}U, ^{232}Th, ^{40}K and ^{235}U in a standard concrete room with thickness of 20 cm. At densities lower than 2350 kg/m^3 a relative decrease in D_A is observed whereas a relative increase is observed at densities higher than 2350 kg/m^3. In case of a density of 1000 kg/m^3 a relative decrease of 34 %, 35 %, 38 % and 20 % is observed for respectively ^{238}U, ^{232}Th, ^{40}K and ^{235}U. In case of a density of 3500 kg/m^3 cm a relative increase of 9 %, 10 %, 11 % and 2 % is observed for respectively ^{238}U, ^{232}Th, ^{40}K and ^{235}U. With increasing densities the total number of radionuclides present in the material will increase leading to higher D_A. With decreasing densities to contrary is true.

With increasing densities the relative contribution of the floor and ceiling to total dose rate decreases with approximately 1 % whereas the dose rate of the walls increases slightly. This effect is observed for the different radionuclides.

3.2.3. Impact of the room size calculated by the EGDA>0% model

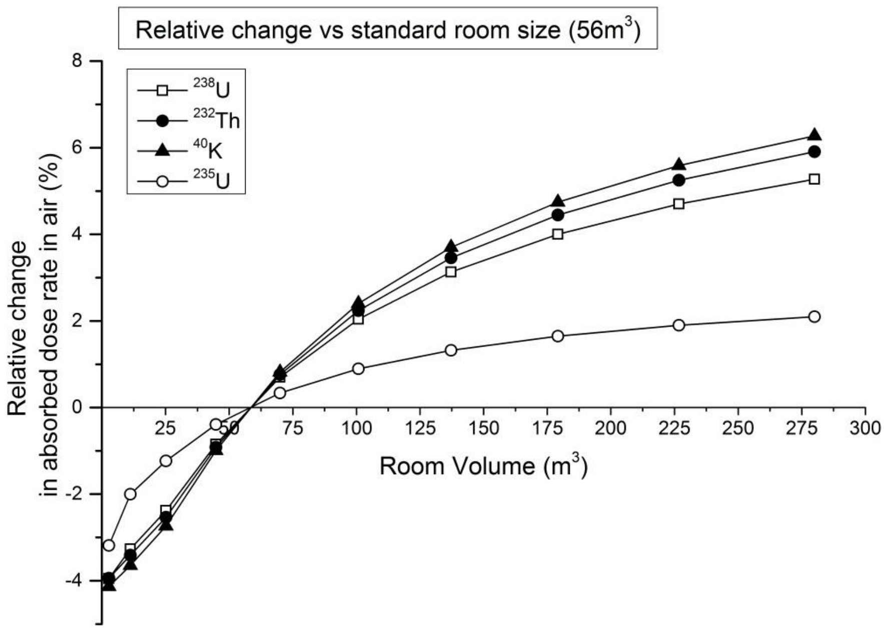

Figure 3: Relative difference of the absorbed dose rate in air for a standard concrete room with varying room size (2.8 - 280 m^3) vs a standard concrete room with room size of 56 m^3 for ^{238}U, ^{232}Th, ^{40}K and ^{235}U.

Figure 3 shows the difference in D_A for different room sizes relative to the standard room size (200 x 250 x 280 cm^3) for ^{238}U, ^{232}Th, ^{40}K and ^{235}U in a standard concrete room. It is observed that the relative decrease in D_A occurs with decreasing room size. In case of a room size of 2.8 m^3 a relative decrease of 4 %, 4 %, 4 % and 3 % is observed for respectively ^{238}U, ^{232}Th, ^{40}K and ^{235}U. In case of a room size of 280 m^3 a relative increase of 5 %, 6 %, 6 % and 2 % is observed for respectively ^{238}U, ^{232}Th, ^{40}K and ^{235}U. With increasing room size to person standing in the room is surrounded by more material. Consequently the total number of radionuclides present in the room will also increase, leading to higher D_A. With decreasing room size the contrary is true.

Figure 3 also shows that the influence of the room sizes affects the radionuclides differently.

Next to changing the room surface the impact of the room height is studied. At small room volumes (below approximately 15 m^3), the D_A of ^{232}Th is lower in case of a height of 200 cm than in case of a height of 280 cm. For a room area of 1 m^2 a difference of approximately 2.3 %, 2.5 %, 2.7 % and 1.2 % difference for respectively ^{238}U, ^{232}Th, ^{40}K and ^{235}U is observed. However at room size larger than 15 m^3 the impact of height on the D_A is reverted. At a room volume of 280 m^3 an increase in the D_A of 1.7 %, 2.0 %, 2.1 % and 0.5 % for respectively ^{238}U, ^{232}Th, ^{40}K and ^{235}U is observed in favour of the room height of 200 cm .

<u>3.2.4 The impact of the presence of windows and doors by the EGDA>0% model</u>

Table 7: % Deviation in dose rate for different window surfaces located in the middle or the corner of Wall 1 (400cmx280cm), Wall 2 (500x280cm) and the ceiling (400 cm x 500cm) in comparison to respectively Wall 1, Wall 2 and the ceiling without the presence of windows.

	Window 100 cm x 100 cm		**Window 100 cm x 200 cm**		**Window 200 cm x 200 cm**	
	Middle	**Corner**	**Middle**	**Corner**	**Middle**	**Corner**
	% Deviation in absorbed dose rate in air (D_A) originating from wall 1 (400 cm x 280 cm) with a window in comparison wall 1 without a window					
^{238}U	-11.8	-7.3	-22.5	-21.1	-43.2	-36.6
^{232}Th	-11.8	-7.3	-22.5	-21.1	-43.1	-36.6
^{40}K	-11.7	-7.4	-22.4	-21.0	-43.0	-36.6
^{235}U	-12.1	-7.2	-23	-21.4	-43.9	-36.7
	% Deviation in absorbed dose rate in air (D_A) originating from wall 2(500 cm x 280 cm) with a window in comparison to wall 2 without a window					
^{238}U	-11.7	-4.5	-21.9	-19.9	-41.1	-26.4
^{232}Th	-11.6	-4.5	-21.8	-19.9	-41.0	-26.4
^{40}K	-11.5	-4.6	-21.7	-19.8	-40.7	-26.4
^{235}U	-12.2	-4.3	-22.6	-20.4	-42.2	-26.1
	% Deviation in absorbed dose rate in air (D_A) originating from a ceiling (500 cm x 400 cm) with a window in comparison to a ceiling without a window					
^{238}U	-14.6	-2.2	-22.8	-6.4	-40.8	-17.3
^{232}Th	-14.4	-2.3	-22.5	-6.4	-40.4	-17.2
^{40}K	-13.9	-2.2	-21.7	-6.3	-39.2	-16.9
^{235}U	-15.7	-2.1	-23.9	-6.1	-42.5	-16.9

Table 7 shows the percentage of deviation in the D_A of the different room components in comparison to the standard concrete room. With increasing size of the window or door surface the D_A of the component decreases. For example, in wall one the D_A decreases with approximately 12 % in case of a window of 100 cm x 100 cm whereas this decrease is approximately 37 % for a window of 200 cm x 200 cm. In both cases the windows are positioned in the middle of wall. Nevertheless the position of the surface in the component plays an important role. In wall 2 the D_A decreases for approximately 41% when the window is positioned in the middle of the wall. When the same window is positioned in the corner, the D_A decreases with 26 % in comparison to a standard concrete room. In addition it must be noted that in the case of a standard concrete room wall 1, wall 2 and the floor/ceiling contribute for approximately 9.5 %, 14.5 % and 26 % respectively to the total D_A of the room. The final influence on the D_A due to the presence of a window in the ceiling will be larger than for a window in wall 1.

3.3 Comparison of index and dose calculations

Table 8: Overview of the index-values and effective dose (mSv/y) of the index and dose calculations used in the European legislative framework for different building materials consisting of residues or cement.

	Index							
Model	**ACI**	**I(pd)**						
Thickness (cm)	20	10	10	18	20	25	40	40
Density (kg/m^3)	2350	1400	3000	3000	2350	1400	1400	3000
Furnace slags	0.788	0.384	0.628	0.811	0.770	0.678	0.822	1.006
Bottom ash and fly ash	1.269	0.609	0.997	1.290	1.225	1.077	1.307	1.602
Phosphogypsum	1.405	0.719	1.171	1.510	1.434	1.264	1.529	1.864
Bauxite residue	3.592	1.657	2.710	3.509	3.330	2.928	3.554	4.355
Cement	0.385	0.180	0.295	0.382	0.363	0.319	0.387	0.476
Scenario number		1	2	3		4	5	6
	Dose (mSv/y)							
Model	**Mark$_{orig}$**	**D(pd)**						
Thickness (cm)	20	10	10	18	20	25	40	40
Density (kg/m^3)	2350	1400	3000	3000	2350	1400	1400	3000
Furnace slags	0.726	0.238	0.549	0.745	0.704	0.606	0.755	0.916
Bottom ash and fly ash	1.293	0.521	1.017	1.329	1.264	1.108	1.346	1.604
Phosphogypsum	1.592	0.659	1.237	1.595	1.521	1.342	1.614	1.905
Bauxite residue	3.825	1.841	3.190	4.043	3.865	3.437	4.087	4.796
Cement	0.206	-0.019	0.128	0.222	0.202	0.155	0.227	0.304
Scenario number		1	2	3		4	5	6
		Dose (mSv/y)						
Model		**EGDA>0%**						
Thickness (cm)		10	10	18	20	25	40	40
Density (kg/m^3)		1400	3000	3000	2350	1400	1400	3000
Furnace slags		0.238	0.557	0.736	0.697	0.590	0.712	0.813
Bottom ash and fly ash		0.520	1.029	1.317	1.254	1.083	1.279	1.441
Phosphogypsum		0.661	1.252	1.577	1.506	1.313	1.533	1.710
Bauxite residue		1.830	3.192	3.971	3.798	3.337	3.868	4.323
Cement		-0.019	0.132	0.219	0.199	0.148	0.207	0.257
Scenario number		1	2	3		4	5	6

Table 8 shows different index and dose values for 5 types of building materials calculated via different models described in Table 2. It must be noted that different authors and models use different background reductions like mentioned in Table 2. In addition in all calculations it is assumed that both the walls as the floor/ceiling have the same density and thickness. The ACI calculation is a non-flexible calculation and assumes a density of 2350 kg/m^3 and walls of 20 cm thick and is considered as a reference for comparison since this is screening tool prescribed by the EU-BSS. Looking at a building material with density of 2350 kg/m^3 and thickness of 20

cm, the index value of the ACI is higher than the index value of I(ρd) except for the phosphogypsum composition.
In case of building materials lighter than 2350 kg/m^3 and thinner than 20 cm building materials, the ACI overestimates the index-value in comparison to I(ρd) (scenario 1). In scenario 2 and 3 the building material is thinner than 20cm and heavier than 2350 kg/m^3. In scenario 2 solely overestimations by the ACI are observed. In scenario 3, an overestimation by the ACI only occurs in case of bauxite residue and cement. In contrast an underestimation occurs in case of furnace slags, bottom and fly ashes and phosphogypsum. In scenarios 4 and 5 the building material is lighter than 2350 kg/m^3 and thicker than 20 cm. In scenario 4, the ACI overestimates the index value in comparison I(ρd). In scenario 5 an overestimation by the ACI occurs in case of bauxite residue. In contrast an underestimation occurs in case of furnace slags, bottom and fly ashes, phosphogypsum and cement. Looking at building materials heavier than 2350 kg/m^3 and thicker than 20 cm, the ACI underestimates the index-value (scenario 6).

In scenario 1 the ACI underestimates the index-value, it is recommended to use the I(ρd) when that ACI index value is above 1. As in scenario 3 and 5 the ACI can over or underestimate the index value it is best to use the I(ρd). As the density and thickness parameters of scenario 2 and 4 correspond to the parameters of scenario 3 and 4 respectively, it is best to also use the I(ρd) for scenario 2 and 4. For scenario 6 the ACI underestimates the index value and from a radioprotection point of view I(ρd) is recommended.

As underestimations by the $Mark_{orig}$ model (corresponds to ACI) in comparison to D(ρd) (corresponds to I(ρd)) occur in scenario 2, 3, 5 and 6, it is recommended from a radioprotection point of view to use the D(ρd) calculation. In other scenarios it is recommended to use the D(ρd) calculation when the effective dose approximates 1mSv/y.

Comparing the D(ρd) with EGDA>0% one can see that the D(ρd)-dose-values are for all scenarios higher than the ones calculated via EGDA>0% except for scenario 1 and 2, which have a low wall thickness. In both scenarios, the EGDA>0% gives an effective dose which is solely a few µSv/y higher. In scenario 3, 4, 5 and 6 the EGDA>0% gives a dose which is from the order of 10 µSv/y to several 100's µSv/y lower. Therefore, in these scenarios, in case of an effective dose close to 1mSv calculated by D(ρd), the authors recommend using a more detailed dose assessment model like EGDA>0% to more accurately assess the dose. It must also be noted that in this comparison the density and thickness of the walls and floor/ceiling are all equal. This can be different in reality and can affect the dose significantly. In addition one has to take into account that a room size larger than 400 cm x 500 cm x 280 cm gives rise to a dose increase like discussed in section 3.2.3. In addition, the presence of windows and doors will also impact this background correction as well as the different sample compositions.

Regarding the different residues, the AC of a residue can vary according to the input, process parameters, etc. [47,48]. Therefore one cannot draw conclusions from the index and dose values of Table 8 on the usage of these classes of residues as building material but a case by case approach should be performed.

4. Conclusion

The current study provides a dose calculation assessment based on the original dose calculation of Markkanen with expanded number of gamma lines and higher total gamma intensity. It is shown that working with averaged gamma lines increases the absorbed dose rate in air for ^{238}U and ^{232}Th with 6.1 % and 0.9 % respectively in case of a standard concrete room. In contrast, a decrease of 4.6 % is determined in case of ^{235}U.

The presence of the build-up increases the absorbed dose rate in air and plays an important role in the final obtained dose received from building materials. In case the build-up is absent, a decrease in absorbed dose rate in air of 52 %, 50 %, 48 % and 67 % for respectively ^{238}U, ^{232}Th, ^{40}K and ^{235}U is observed. In case of the ISS_{Pelli} model, the use of the Pelliccioni Berger parameters lowered the absorbed dose rate in air with 2.8 % and 2.6 % for respectively ^{238}U and ^{232}Th in comparison with the ISS_{orig} model, which uses the Berger parameters described by Markkanen. Further improvements on the accuracy of the B and consequently the absorbed dose rate in air can be made by working with build-up factors customized towards the chemical composition of the building material with for example a geometric progression approach [49].

The developed EGDA>0% model is complementary to the existing ACI/original Markkanen model and I(ρd)/D(ρd) index/dose calculations which prove relevant for the dose assessment within the European legislative framework applicable towards building materials. Due to its simplicity the authors recommend to perform a first screening by using the ACI proposed by the EU-BSS in the case of building materials thinner than 20 cm or lighter than 2350 kg/m^3. In the case of a building material thicker than 20 cm or heavier than 2350 kg/m^3, the authors propose to use D(ρd) calculation tool of Nuccetelli et al. [2] in case of standard room sizes. In case the resulting dose of this calculation exceeds 1 mSv/y one should perform a more detailed dose assessment. The EGDA>0% model can be used for these specific cases. The EGDA>0% model also allows coping with non-standard room sizes or the presence of doors and windows The model does not consider the dose originated by 222Rn exhalation resulting in an overestimation of the total external gamma dose originating from building materials.

A sensitivity analysis was performed of the EGDA>0% model. The main factors that contribute to increase the absorbed dose rate in air in comparison to a standard concrete room (Volume of 56 m^3; density of 2350kg/m^3; wall/floor/ceiling thickness of 20 cm) are

- Increasing density; in case of 3500 kg/m^3 an increase of 9 %, 10 %, 11 % and 2 % for respectively ^{238}U, ^{232}Th, ^{40}K and ^{235}U is observed.
- Increasing thickness; in case of 80 cm thick walls an increase of 6 %, 7 %, 8 % and 1 % for respectively ^{238}U, ^{232}Th, ^{40}K and ^{235}U is observed.
- Increasing volume; in case of a room volume of 280 m^3 an increase of 5 %, 6 %, 6 % and 2 % for respectively ^{238}U, ^{232}Th, ^{40}K and ^{235}U is observed.

The main factors that contribute to decrease the absorbed dose rate in air in comparison to a standard concrete room are:

- Decreasing density; in case of 1000 kg/m^3 a decrease of 34 %, 35 %, 38 % and 20 % for respectively ^{238}U, ^{232}Th, ^{40}K and ^{235}U is observed.
- Decreasing thickness; in case of 5 cm thick walls a decrease of 27 %, 28 %, 29 % and 21 % for respectively ^{238}U, ^{232}Th, ^{40}K and ^{235}U is observed.
- Decreasing volume; in case of a volume of 2.8 m^3 a decrease of 4 %, 4 %, 4 % and 3 % for respectively ^{238}U, ^{232}Th, ^{40}K and ^{235}U is observed.
- Presence of windows or doors; in case of one window of 2 x 2 m in wall 1 a decrease of 4 % for ^{238}U, ^{232}Th, ^{40}K and ^{235}U is observed.

In addition, the shape of the room can also impact the absorbed dose rate in air. Also the position and size of the window or door in the wall will impact the final absorbed dose rate in air. Larger windows positioned in the middle of the wall lead to a lower absorbed dose rate in air. The implementation of the chemical composition in the model via the attenuation coefficients showed limited effects on the absorbed dose rate in air. For a standard room an increase of 1.4 %, 0.9 % and 2.1 % is observed for ^{238}U, ^{232}Th and ^{40}K in case of a FSIP sample composition in comparison to a concrete sample composition. In contrast, a decrease of 6.8% in case of ^{235}U is observed.

Although the Markkanen room model is widely spread and used as a conservative screening tool in European legislation, the uncertainty of the method should be assessed. The expansion proposed here expands the model with validated scientific date but does not take care of the uncertainty. The uncertainty assessment is a topic for further research.

Acknowledgement

This work was supported by the COST Action TU1301. www.norm4building.org.

References

[1] M. Markkanen, Radiation Dose Assessments for Materials with Elevated Natural Radioactivity, Finish Cent. Radiat. Nucl. Safety. Rep. STUK-B-STO 32. (1995) 1–41.

[2] C. Nuccetelli, F. Leonardi, R. Trevisi, A new accurate and flexible index to assess the contribution of building materials to indoor gamma exposure, J. Environ. Radioact. 143 (2015) 70–75. doi:10.1016/j.jenvrad.2015.02.011.

[3] United Nations, Sources and Effects of Ionizing Radiation United Nations Scientific Committee on the Effects of Atomic Radiation UNSCEAR 2000 Report to the General Assembly, with Scientific Annexes VOLUME I: SOURCES, 2000.

[4] European Council, Laying down basic safety standards for protection against the dangers arising from exposure to ionising radiation, and repealing directives 89/618/Euratom, 90/641/Euratom, 96/29/Euratom, 97/43/Euratom and 2003/122/Euratom, Off. J. Eur. Union. (2014) 1–73.

[5] European Commission, A resource-efficient Europe - Flagship initiative under the Europe 2020 Strategy, (2011).

[6] European Commission, A strategy for smart, sustainable and inclusive growth, (2010).

[7] European Commission, Roadmap to a resource efficient Europe, (2011).

[8] W. Schroeyers, T. Croymans-Plaghki, S. Schreurs, Towards a holistic approach for risk assessment when reusing slag with enhanced NORM content in building materials, 4th Int. Slag Valoris. Symp. (2015).
[9] Y. Pontikes, R. Snellings, Cementitious binders incorporating residues, in: Handb. Recycl., 2014: p. 219–229. doi:10.1016/B978-0-12-396459-5.00016-7.
[10] C. Nuccetelli, Y. Pontikes, F. Leonardi, R. Trevisi, New perspectives and issues arising from the introduction of (NORM) residues in building materials: A critical assessment on the radiological behaviour, Constr. Build. Mater. 82 (2015) 323–331. doi:10.1016/j.conbuildmat.2015.01.069.
[11] R. Siddique, I.M. Khan, Supplementary Cementing Materials, 2011. doi:10.1017/CBO9781107415324.004.
[12] D.V. Ribeiro, J.A. Labrincha, M.R. Morelli, Use of Calcined Bauxite Waste as a Supplementary Cementitious Material: Study of Pozzolanic Activity, J. Mater. Sci. Eng. 4 (2014) 172–178.
[13] T. Croymans, I. Vandael Schreurs, M. Hult, G. Marissens, L. Guillaume, H. Stroh, S. Schreurs, W. Schroeyers, Variation of natural radionuclides in non-ferrous fayalite slags during a one-month production period, J. Environ. Radioact. (2016).
[14] R. Trevisi, S. Risica, M. D'Alessandro, D. Paradiso, C. Nuccetelli, Natural radioactivity in building materials in the European Union: A database and an estimate of radiological significance, J. Environ. Radioact. 105 (2012) 11–20. doi:10.1016/j.jenvrad.2011.10.001.
[15] L. Koblinger, Calculation of exposure rates from gamma sources in walls of dwelling rooms, Health Phys. 34 (1978) 459–463.
[16] E. Stranden, Radioactivity of building materials and the gamma radiation in dwellings, Phys. Med. Biol. 24 (1979) 921–930.
[17] S. Righi, S. Verità, P.L. Rossi, M.F. Maduar, A dose calculation model application for indoor exposure to two-layer walls gamma irradiation: the case study of ceramic tiles, Radiat. Prot. Dosimetry. 171 (2016) 545–553. doi:10.1093/rpd/ncv476.
[18] P. de Jong, W. van Dijk, Modeling gamma radiation dose in dwellings due to building materials., Health Phys. 94 (2008) 33–42. doi:10.1097/01.HP.0000278509.65704.11.
[19] J. Deng, L. Cao, X. Su, Monte Carlo simulation of indoor external exposure due to gamma-emitting radionuclides in building materials, Chinese Phys. C. 38 (2014) 108202. doi:10.1088/1674-1137/38/10/108202.
[20] M. Zeeshan Anjum, S.M. Mirza, M. Tufail, N.M. Mirza, Z. Yasin, Natural radioactivity in building materials: dose determination in dwellings using hybrid Monte Carlo-deterministic approach, Int. Conf. Nucl. Data Sci. Technol. (2007) 1–4. doi:10.1051/ndata:07187.
[21] N.M. Mirza, S. Mirza, A Shape and Mesh Adaptive Computational Methodology for Gamma Ray Dose from Volumetric Sources, Radiat. Prot. Dosimetry. 38 (1991) 307–314. doi:10.1093/oxfordjournals.rpd.a081106.
[22] R. Mustonen, Methods for evaluation of doses from building materials, Radiat. Prot. Dosimetry. 7 (1984) 235–238.
[23] C. Nuccetelli, S. Risica, M.D. Alessandro, R. Trevisi, Natural radioactivity in building material in the European Union : robustness of the activity concentration index I and comparison with a room model, J. Radiol. Prot. 32 (2012) 349–358. doi:10.1088/0952-4746/32/3/349.
[24] V. Manić, G. Manić, D. Nikezic, D. Krstic, Calculation of Dose Rate Converstion Factors

for 238U, 232Th and 40K in Concrete Structures of Various Dimensions, With Application To Nis, Serbia, Radiat. Prot. Dosimetry. 152 (2012) 361–368.

[25] V. Manić, D. Nikezic, D. Krstic, G. Manić, Assessment of indoor absorbed gamma dose rate from natural radionuclides in concrete by the method of build-up factors, Radiat. Prot. Dosimetry. 162 (2014) 609–617. doi:10.1093/rpd/nct358.

[26] B. Chen, Q. Wang, W. Zhuo, Assessment of gamma dose rate in dwellıngs due to Decoratıve stones., Radiat. Prot. Dosimetry. 166 (2015) 1–4. doi:10.1093/rpd/ncv256.

[27] S. Risica, C. Bolzan, C. Nuccetelli, Radioactivity in building materials: room model analysis and experimental methods., Sci. Total Environ. 272 (2001) 119–126.

[28] European Commission, Radiation protection 112 Radiological protection principles concerning the natural radioactivity of building materials, (1999) 1–16.

[29] R. Mustonen, Methods for evaluation of radiation from building materials, Radiat. Prot. Dosimetry. 7 (1985) 235–238.

[30] European Commission, Radiation protection 122 practical use of the concepts of clearance and exemption Part II application of the concetps of exemption and clearance to natural radiation sources, 2002.

[31] Laboratoire national Henri Becquerel, Decay Data Evaluation Project, (2016). http://www.nucleide.org/DDEP.htm (accessed May 22, 2016).

[32] NIST, Composition of Concrete, Portland, (n.d.) 1. http://physics.nist.gov/cgi-bin/Star/compos.pl?matno=144.

[33] J.E. Martin, Physics for radiation protection, WILEY-VCH Verlag GmbH & Co. KGaA 2nd Edition, 2006.

[34] J.H. Hubbell, S.M. Seltzer, Tables of x-ray mass attenuation coefficients and mass energy-absorption coefficients 1 keV to 20 meV for elements z = 1 to 92 and 48 additional substances of dosimetric interest, 1995.

[35] M. Pelliccioni, Fondamenti fisici della radioprotezione, Pitagora, 1989.

[36] D. Krstic, D. Nikezic, Calculation of Indoor Effective Dose factors in Ornl Phantoms Series Due to Natural Radioactivity in Building Materials, Health Phys. 97 (2009) 299–302.

[37] R Devellopment Core Team, R: A language and environment for statistical computing. R Foundation for Statistical Computing, Vienna, Austria., (2008). http://www.r-project.org.

[38] J.H. Hubbell, Photon mass attenuation and energy-absorption coefficients, Int. J. Appl. Radiat. Isot. 33 (1982) 1269–1290.

[39] M.J. Berger, J.H. Hubbell, S.M. Seltzer, J. Chang, J.S. Coursey, R. Sukumar, D.S. Zucker, K. Olsen, XCOM: Photon Cross Sections Database, NIST Stand. Ref. Database 8. (2010) 1–5. http://www.nist.gov/pml/data/xcom/.

[40] IAEA, NuDat, (n.d.). http://www.nndc.bnl.gov/nudat2/.

[41] L. Kriskova, P.T. Jones, H. Jannsen, B. Blanpain, Y. Pontikes, Synthesis and Characterisation of Porous Inorganic Polymers from Fayalite Slag., Slag Valoris. Symp. Zero Waste. 4 (2015) 227–230.

[42] S. Onisei, K. Lesage, B. Blanpain, Y. Pontikes, Early Age Microstructural Transformations of an Inorganic Polymer Made of Fayalite Slag, J. Am. Ceram. Soc. 9 (2015) 1–9. doi:10.1111/jace.13548.

[43] R.I. Iacobescu, V. Cappuyns, T. Geens, L. Kriskova, S. Onisei, P.T. Jones, Y. Pontikes, The influence of curing conditions on the mechanical properties and leaching of inorganic polymers made of fayalitic slag, Front. Chem. Sci. Eng. (2017) 208–213.

doi:10.1007/s11705-017-1622-6.

[44] M. Berger, J. Hubbell, XCOM: Photon cross sections on a personal computer, Natl. Bur. Stand. Washington, DC (USA). Cent. Radiat. Res. (1987) 1–28. doi:10.2172/6016002.

[45] M. Marangoni, L. Arnout, L. Machiels, L. Pandelaers, E. Bernardo, P. Colombo, Y. Pontikes, C. Jantzen, Porous, Sintered Glass-Ceramics from Inorganic Polymers Based on Fayalite Slag, J. Am. Ceram. Soc. 99 (2016) 1–7. doi:10.1111/jace.14224.

[46] T. Hertel, B. Blanpain, Y. Pontikes, A Proposal for a 100 % Use of Bauxite Residue Towards Inorganic Polymer Mortar, J. Sustain. Metall. 2 (2016) 394–404. doi:10.1007/s40831-016-0080-6.

[47] IAEA, Extent of Environmental Contamination by Naturally Occurring Radioactive Material (NORM) and Technological Options for Mitigation - Technical reports series no. 419, 2003.

[48] T. Croymans, I. Schreurs, M. Hult, G. Marissens, H. Stroh, G. Lutter, S. Schreurs, W. Schroeyers, Variation of natural radionuclides in non-ferrous fayalite slags during a one-month production period, J. Environ. Radioact. 172 (2017) 63–73. doi:10.1016/j.jenvrad.2017.03.004.

[49] Y. Harima, Validity of the Geometric-Progression Formula in approximating Gamma-Ray Buildup Factors, Nucl. Sci. Eng. 5 (1986) 24–35.